Advanced Ceramics Progress

Research Article

Optimization of Heat Treatment Cycles in Sub-atmospheric LiF-NaF-KF Based Fluoride Ion Cleaning for Removing Oxide Layers in Cracks of IN738-LC

S. Hamidi [a], M.R. Rahimipour [a], M.J. Eshraghi [b] *, H. Esfahani [c]

[a] Department of Ceramics, Materials and Energy Research Center (MERC), Meshkindasht, Alborz, Iran
[b] Department of Semiconductors, Materials and Energy Research Center (MERC), Meshkin Dasht, Alborz, Iran
[c] Department of Materials Engineering, Bu-Ali Sina University, Hamedan, Hamedan, Iran

A B S T R A C T

An improved Fluoride Ion Cleaning (FIC) process required for removing all oxide layers by a molten mixture of alkaline fluoride salts under sub-atmospheric pressure was developed and applied to oxide layers on the cracks formed on the surface of Inconel 738-LC samples. This method is directly characterized by filling up the cracks with a molten mixture of alkaline fluoride salts (LiF-NaF-KF) overheated under sub-atmospheric pressure and subsequently, by injecting hot hydrogen gas into the process chamber. The effect of cleaning time on the microstructure of the finished surface was studied in time durations up to 120 min in intervals of 30 min using cross-sectional micrographs and elemental distribution maps. In accordance with the amount of mass loss and microstructural studies during the cleaning process, the optimum cleaning time was suggested to be 90-120 min. Perquisite microstructural outcome shows that in the suggested cleaning condition, all oxide scales in the cracks would be removed without any extra damage to the gamma prime depleted layer, which is a necessary layer for preventing sample oxidation before repair. In this regard, subsequent brazing operations need an oxide-free surface.

1. INTRODUCTION

Nickel-based superalloys are known for their mechanical strength and high corrosion resistance at high temperatures which would cause fatigue micro-cracks [1,2]. On the contrary, the relatively high-temperature oxidation resistance of these superalloys is due to the formation of dense oxides of Cr_2O_3, TiO_2, Al_2O_3, and $NiCr_2O_4$ spinel [3,4]. To reuse these superalloys, it is necessary to perform an expansive process of removing oxide films formed on the surface, especially those created in the micro-cracks.

Fluoride compounds are widely used as chemical agents for removing ceramic oxide layers due to their high chemical reactivity and electronegativity [5]. There are three common types of Fluoride Ion Cleaning (FIC) methods for removing the oxide films: (i) chrome fluoride-based systems such as CrF_3 and $NH_4F + Cr$; (ii) fluorocarbon-based systems such as PTFE; and (iii) mixed gas systems such as HF and H_2 [6-8]. In 1991, Kim et al. [9] proposed a variation of the FIC process in which cleaning was performed at sub-atmospheric pressure by injecting HF gas into the process chamber. They showed that upon reducing the chamber pressure to sub-atmospheric levels before HF injection, deep penetration of the reductant gases into the cracks would increase that results in the oxide film removal. In 2006, Miglietti et al. [10] used the thermal decomposition of Poly Tetra Fluoro Ethylene (PTFE) grease in the atmosphere in order to clean the superalloy oxides. They detected concentrated

---

oxygen in the specimen surface after the cleaning process. According to their study, the gas-based method enjoys several benefits including precise process controllability and risk assessment with regard to hazardous HF gas; however, its disadvantages such as process complexity and high instrument costs give industries and researchers the incentive to look for safer and less expensive methods.

Therefore, the development of the promoted methods with less complexity and hazards than gas-based methods for removing oxides from the narrow cracks is still desirable. The proposed method in this research comprises a combination of processes for both solid- and gas-based methods. To this end, the present study proposes a new method by implementing the following three stages: (i) filling up the cracks with alkaline fluoride salts after the cleaning process in a clean environment, (ii) heating up the process in a clean chamber in sub-atmospheric pressure up to the melting point of alkaline fluoride salts, and (iii) injecting hydrogen at atmospheric pressure. The proposed method for cleaning cracks in this study is a combination of pressure reduction and molten fluorine salt in addition to hydrogen injection in the chamber during the process. Among the advantages of such a method are the safety and environmentally friendliness of alkaline fluoride salts in comparison to HF gas used in the usual FIC process. Reducing the temperature during the process is also beneficial since high temperature would cause damage to the gamma prime depletion layer and structural disorder [11]. Therefore, using salts at a low melting point facilitates the remaining alloy composition and phases during the process that is done in reducing the atmosphere. In order to achieve a low melting point, low viscosity, and low volatility salts, the ternary systems of alkaline fluoride salts were taken. According to the literature [12-14], the eutectic mixture of three fluoride salts (29.3 % LiF-11.6 % NaF- 59.1 % KF (wt. %)) at a melting point of 454˚C was chosen, being well suited for the temperature range for the proposed desired method.

The novlty of this research lies in its usage of a less hazardous solid fluoride source used in the vacuum chamber. As mentioned earlier, performing the process with a reduced pressure could improve the penetration of the molten fluorine salt into the cracks and help remove oxides in the depth of cracks. In addition, introducing hydrogen which is a reducing agent and acts as an activator for fluorine salt to produce hydrogen fluoride gas at the local positions is another key factor associated with the proposed method. To the best of the authors' knowledge, there has been no report on injecting hydrogen gas to a vacuum chamber to simultaneously perform the FIC process via molten fluoride salts. Another benefit of this method is that using fluoride salts on the local oxide scales leaves other parts unattacked. However, the flow of hydrogen in the chamber removes the reaction byproducts and allows newly generated hydrogen fluoride to act on the remaining oxide. As mentioned earlier, the FIC process was completed in Stage (iii) and for optimization, the experimental condition in Stages (i) and (ii) was fixed; however, the effects of soaking time in Stage (iii) on removing oxides from the cracks were systematically investigated using cross-sectional micrographs and elemental distribution maps.

2. MATERIALS AND METHODS

2.1. Sample and Crack Preparation

The chemical composition of the selected alloy (IN-738LC) is reported in Table 1. Specimens were prepared in a plate with dimensions of 10 mm × 10 mm × 4 mm. Microcracks were formed by an NC wire Electro-Discharge Machining (EDM). The surfaces of the samples were polished using 600 up to 2000 grades of SiC paper and subsequently, sonicated in acetone for 15 minutes to clean the surface from SiC polishing contamination. According to our previous study on oxidation kinetics [14], the oxidation at 950 °C over 160 hours does not tend to form an oxide layer with a much higher thickness on top of Ni-based superalloy. Therefore, the oxide layers were formed by holding samples at 950 °C in the ambient atmosphere for 160 hours.

TABLE 1. Chemical composition of superalloy used in this study

Elemental	Ni	Cr	Co	Ti	Al
wt. %	Base	15	9.5	3.6	3.5
Elemental	W	Mo	Ta	Nb	C
wt. %	3.2	1.7	1.5	1.0	0.1

2.2. Cleaning procedure

The cleaning procedure begins in Stage (i) in which the samples are embedded in a 4g mixture of alkaline fluoride salts as a chemical reactant. This salt comprises LiF (Merck No.: 232-152, purity ≥ 99.99 %), NaF (Merck No.: 231-667-8, purity ≥ 99.5 %), and KF (Merck No.: 232-151-5, purity ≥ 99.0 %) at ratios of 29.3, 11.6, and 59.1 (wt. %), respectively. This ratio has been chosen as FLiNaK for its low melting temperature [15].

Stage (ii) begins by inserting the sample in the reactor and reducing the pressure of the reactor to 3×10^{-3} mbar, while simultaneously increasing the reactor temperature up to 500 °C. In this stage, the alkaline salt is melted and encapsulated in the sample and it fills the cracks. While the reactor is enriched by F- atoms during heat treatment, there is high affinity to other elements that could be formed [16]. Finally, heat treatment continues upon increasing the reactor temperature up to 950 °C and

increasing the reactor pressure up to the atmosphere by injecting hydrogen gas. After finishing the dedicated thermo-chemical regime, the furnace is cooled down to room temperature in a hydrogen atmosphere.

To investigate the effectiveness of the aforementioned procedure in the quality of surface and crack cleaning, samples were analyzed after 30, 90, 60, and 120 min of heat treatment. The samples removed from the furnace were immersed in 0.5 M sulfuric acid for 20 min to wash out the reaction products and by-products from the cracks. The parameters used in Stages (ii) and (iii) are presented in Table 2.

TABLE 2. Time schedule cleaning cycle

Stage	Temperature (°C)	Heating Rate (°C.h^{-1})	Time (min)
(ii)	25-500	600	47.5
(iii)	500-700	150	80
(iii)	700-950	300	30
(iii)	950	-	30,60,90,120

2.3. Characterization

The mass change of the samples after cleaning was measured using a high-precision balance with the accuracy of ± 0.01 milligrams at 23 ± 2 °C. The cross-section of the sample was electrolytically polished with a 12 mL H_3PO_4, 47 ml H_2SO_4, and 16ml CrO_3 solution by applying 3V polarization for 3 s [14]. The phases formed on the surface were analyzed before and after oxidation by X-ray diffractometry (Siemens Model; D500 using Cu-kα radiation). X'pert HighScore Plus software (2.2b) was used to identify these phases. The concentration profiles across the cracks before and after cleaning procedures were examined by Energy Dispersive X-ray Spectrometry (EDS) using spot scan mode in FESEM (model T-scan by 15 kV accelerating voltage). To study the micrographs ImageJ, 1.38x NIH USA was employed.

3. RESULTS AND DISCUSSION

3.1. Characterization of oxide film

Figure 1 presents the X-ray diffraction patterns of samples before and after oxidation at 950 ˚C for 160 h. The XRD pattern of the oxidized sample shows that in the oxide layers, not only single oxide phases such as Al_2O_3 (standard JCPDS card 00-004-0875) Cr_2O_3 (standard JCPDS card 00-038-1479) and a small amount of TiO_2 (standard JCPDS card 01-072-1148) were formed, but also complex oxides such as $NiAl_2O_4$ (standard JCPDS card 00-010-0339) and $NiCr_2O_4$ (standard JCPDS card 00-023-1271) were presented [14].
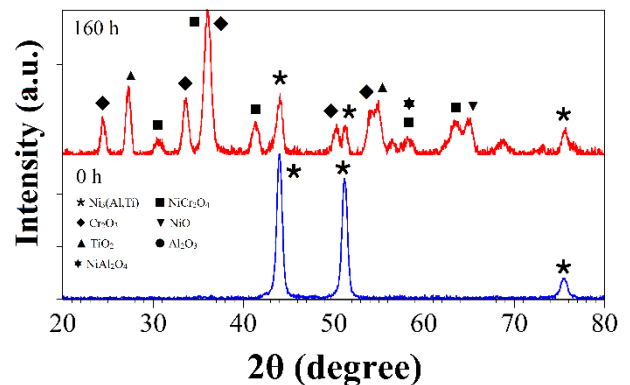

Figure 1. X-ray diffraction patterns of IN-738LC (a) before and (b) after oxidation in air at 950°C for 160 h

Figure 2 shows the microstructural and elemental maps of a typical crack in a sample oxidized at 950 ˚C for 160 h. The fine dot-like feature at the interior depth is attributed to the gamma prime phase [17,18]. This morphology is different in the region near the surface due to the rearrangement of alloy elements during oxidation. The decomposition of gamma prime occurred due to the outward diffusion of Ti and Al to the surface and their reaction with oxygen to form selective oxidation. Furthermore, elemental maps indicate migration of Al, Cr, and Ti alloy elements from different depths and concentrations in the region near the surface. Each element concentrated at a specific distance from the surface can be observed in the regular formation of oxide components during oxidation.

According to the overlay elemental map analysis of the layers, the outer layer mainly consists of TiO_2, Al_2O_3, and small amount of NiO, and the inner layer is composed of Cr_2O_3. However, $NiCr_2O_4$ spinel phase is formed between the outer and inner layers, i.e., the middle layer. Al maps with EDS analysis confirm the formation of Al_2O_3 as the innermost layer because of the higher tendency of aluminum to react with oxygen rather than other elements of the alloy [19, 20].

A relatively thick area is also located between the substrate and internal layers attributed to the gamma prime depleted zone. By extending the oxidation time, elements such as Ni, Cr, and Ti would continue to migrate from these regions to the outer layer to form oxide compounds.

3.2. Cleaning the oxide from the surface of the crack

Figure 3 shows the cross-section micrographs from the cracks of the oxidized samples obtained by an optical microscope and the samples were cleaned for 90 min in the modified FIC process. According to this micrograph,
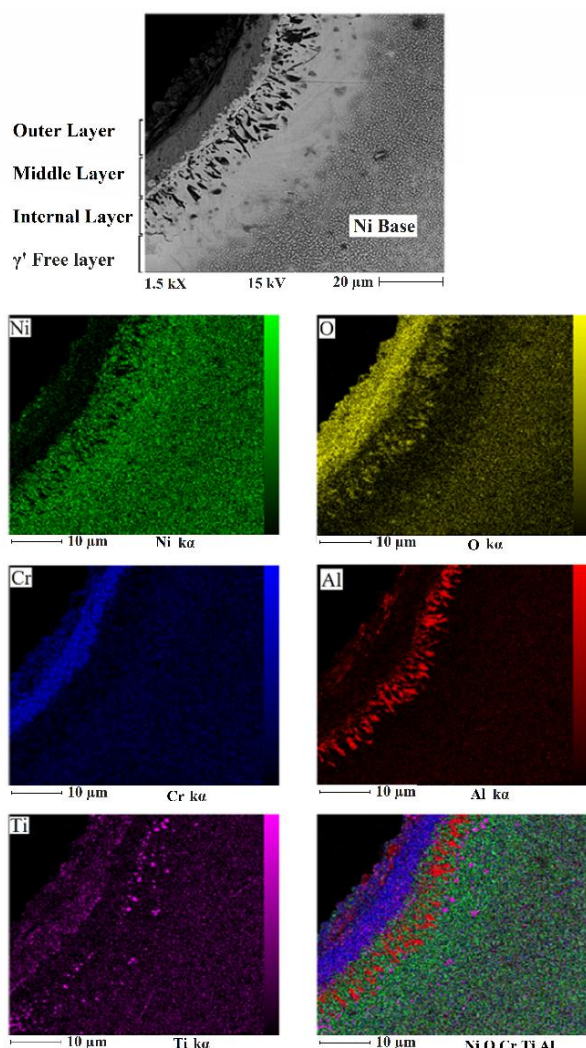
Figure 2. Elemental distribution map of a typical crack in a sample oxidized at 950 ˚C for 160 h

degradation of the base alloy. Therefore, calculation of the mass loss of the sample during the cleaning process and cross-sectional imaging of surface area play significant roles in determining the optimum duration of the FIC process.
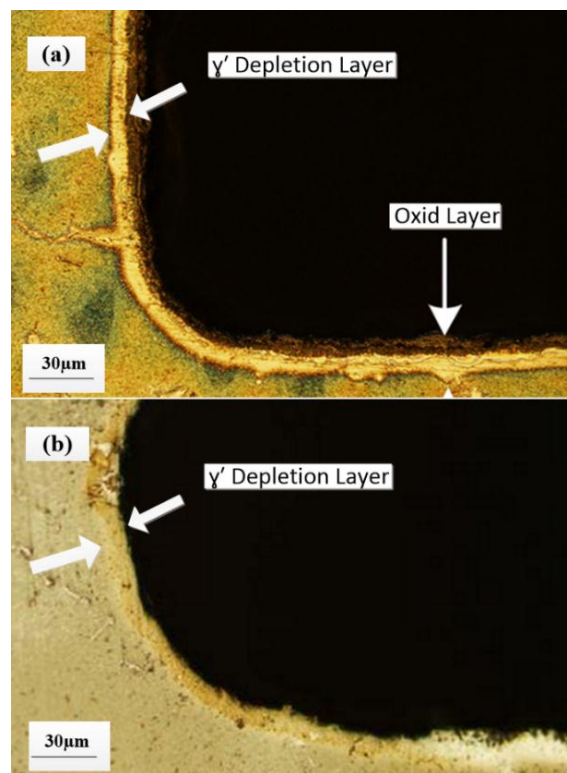

Figure 3. Optical micrographs of (a) sample oxidized for 160 h and (b) sample oxidized and cleaned for 90 min by modified FIC process

the alkaline fluoride salts were removed from the crack surface after completion of stage (iii) of the FIC process. The obtained results showed that alkaline salt could be melted, encapsulated in the microcracks during the Stage (ii), and then, the cleaning condition would suffice to gasify the alkaline fluoride salts during the Stage (iii). A distinct white layer observed in both samples shows the gamma prime depleted area; however, there is a major difference between the locations of this layer in the cleaned and oxidized samples. Although the gamma prime depleted area for the oxidized sample is placed under the oxidized region, as shown in Figure 2, for the cleaned sample, it is located on the surface. The 90 min FIC process can clean the oxide films and retain a metallic surface without any ceramic phases. However, applying the process for increased duration may expose the sample to more attacks which would result in

After removing the oxide films from the surface, the total mass of the sample is expected to be reduced. Figure 4 shows the mass loss per surface area of IN738 LC during the FIC cleaning process or different durations of 30, 60, 90, and 120 min. According to the mass grain duration and 160 h of oxidation [14] as well as Figure 4, the amount of mass loss increased upon increase in the process duration, indicating the removal of oxide films from the surface and corrosion of the substrate. Since the molten salt would possibly diffuse into the metallic area and degrade alloy elements (Al, Ti) causing damage to the base superalloy, it is necessary to study the cross-sectional image of cleaned samples at various cleaning times to determine the optimum progress of the process.
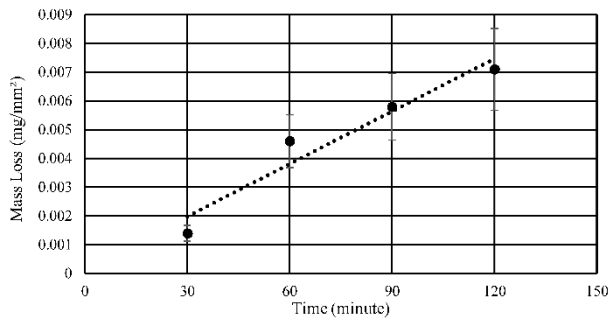
Figure 4. Mass loss per surface area of IN738 LC during FIC cleaning process at 950 °C

The cross-sectional images of a cleaned crack presented in Figure 5 provide significant information on morphology changes during the cleaning process. Figure 5a shows a backscattered electron micrograph of the sample cleaned by the FIC process for 30 min. According to this figure, the FIC process for 30 minutes was not enough to completely remove oxide films; therefore, Cr_2O_3 and Al_2O_3 rich layers corresponding to the middle and internal layers still remained on the surface. According to Figure 5b, increasing the cleaning time to 60 minutes would remove most of the Cr_2O_3 layers. In addition, the number of the dark spots corresponding to Al_2O_3 in the internal layer was reduced to indicate the ability of the salts to diffuse into the sub-layer and clean some of the oxide layers. Most of oxide layers on the surface sample were removed by the process after about 90 minutes with a retaining gamma prime depleted area on top of the samples under the oxide layer (Figure 5c), implying that during the cleaning of the oxides, Ti and Al diffuse outward from the volume into the surface and finally react with the HF, thus deepening the gamma prime depleted area. This depletion promotes the removal of such strong oxide formers near the surface that could boost prevention of oxidation at a stage between cleaning and repairing [21], thus increasing the bonding strength during the repairing process. Increasing the cleaning process up to 120 min would not only remove the entire oxide layer but also clean the gamma prime depleted area (Figure 5d), mainly due to the fact that in the absence of the oxide layer, depleted gamma prime could easily react with salt. It can be concluded that the optimum condition for recovering the samples typically oxidized at 950 °C for 160 h could be performed at 950 °C by soaking in H_2 gas in a time period of 90 to 120 min.

As discussed earlier, at the final stage of the FIC process, the alloying elements may diffuse outward and react with HF, and this behavior gains significance while recognizing the optimum conditions for obtaining the desired surface. According to results, in the process of cleaning the samples for 90 minutes by the modified FIC

process, the elemental depletion was likely to occur. Figure 6 shows the elemental distribution maps for Ni, Al, Ti, Cr, and O within the region near the surface of the crack cleaned by 90 minutes in the modified FIC process. The elemental map also depicts a uniform distribution for Cr, Al, and Ni.
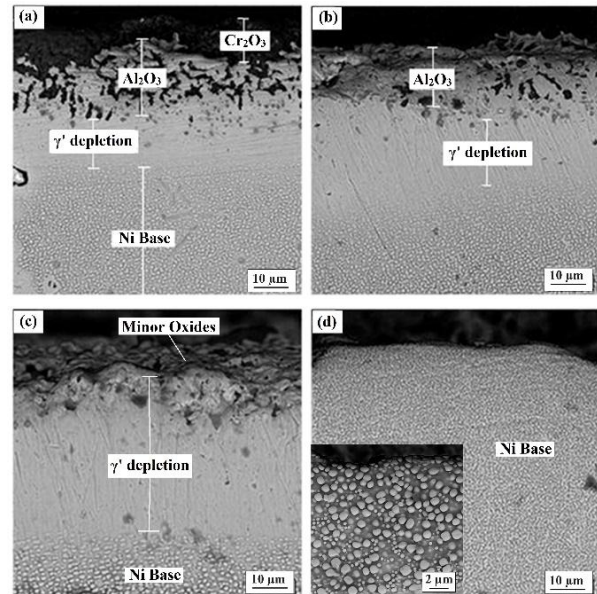

Figure 5. Cross-sectional SEM micrographs of typical crack cleaned by FIC process at 950 ℃ at different times: (a) 30, (b) 60, (c) 90, and (d) 120 min

3.3. Mechanism

The mechanism for the mentioned cleaning procedure, which is a combination of several methods, could be described as follows: In the second stage, fluoride salts reacted with oxide films on the surface at 500 ℃ [22]. The salts indirectly reacted with oxide films step by step. In the beginning, Alkaline salts reacted with the remaining H_2O in a pack of salts to form the HF, as shown in the following [23]:

$$LiF_{(l)} + H_2O_{(g)} = Li_2O_{(g)} + 6LiF_{(g)} \qquad (1)$$
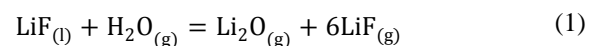
Then, HF reacted, as shown in Eq. 2, with oxide film to form volatile fluoride elements (e.g. for Al_2O_3). The main residues of HF and surface metal oxides reacted are AlF_3 (g), CrF_3 (s), TiF_4 (g), and H_2O (g) [24]. The resultant H_2O may react again with the remainig salts to form more HF reducer agents [25,26].

$$6HF_{(g)} + Al_2O_{3(s)} = 2ALF_{3(g)} + H_2O_{(g)} \qquad (2)$$

Reducing the reactor pressure to sub-atmospheric pressure would make Eq. 1 accelerate in accordance with

the Levine's principle [27]. Therefore, this stage should be performed at a pressure reduced to approximately 1 to 3×10^{-3} mbar. Furthermore, sub-atmospheric pressures forced the gaseous products out of the cracks and were replaced by new HF gas [28]. Therefore, from the thermodynamic point of view, the cleaning process would be accomplished at Stage (ii), in contrast to the kinetic view, suggesting that the cleaning reaction of each oxide could be completed at different times [29].

Stage (iii): To complete the cleaning reactions, H_2 gas was injected into the reactor until the reactor pressure would reach 1013 mbar. The temperature of the reactor was simultaneously increased up to 950 ℃. The injected H_2 gas reacted with the remaining alkaline salts and volatile fluoride element to form an HF cleaning agent, as shown in the following reactions [30]:

$$H_{2(g)} + LiF_{(l)} = HF_{(g)} + LiH_{(g)} \tag{3}$$

$$\tfrac{3}{2}H_{2(g)} + AlF_{3(g)} = Al_{(l)} + 3HF_{(g)} \tag{4}$$
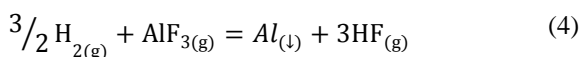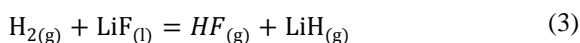
The produced HF gas induced and accelerated the Reaction (2), especially for Cr_2O_3 and TiO_2 [26]. Prolonged heating time would result in the reaction of oxides with HF, thus converting them to their volatile fluorides and evaporating the volatile fluorides. In addition, prolonged heating would result in the diffusion of metal alloy elements outwards and surface depletion by HF reactions with strong oxide formers drawn onto the surface by diffusion.

4. CONCLUSION

The process of the modified fluoride ion cleaning using FLiNaK (29.3%LiF-11.6%NaF-59.1%KF (wt. %)) alkaline salt in sub-atmospheric pressures was investigated in this study in order to effectively remove oxides on the artificial cracks of oxidized Inconel samples. In the modified process, FLiNak was directly plugged into the cracks in the powder form before processing. This method was a combination of methods, i.e., pressure reduction and molten fluorine salt in addition to hydrogen injection in the chamber during the process. The study of the effect of FIC process duration from 30 to 120 minutes at 30-minute intervals showed that the cleaning conditions set as 950 ℃, 90-120 min under H_2 gas were suitable for removing all oxide films, even from the cracks without causing any damage to the base alloy. Increasing the process time to more than 90 minutes would result in corrosion of the base superalloy. The results of the analysis revealed that in an optimum cleaning condition, all oxide films were removed from the surface of the cracks and also, alloy elemental

depleted area was not observed on the final surface. No evidence on the inter-granular attack was observed.
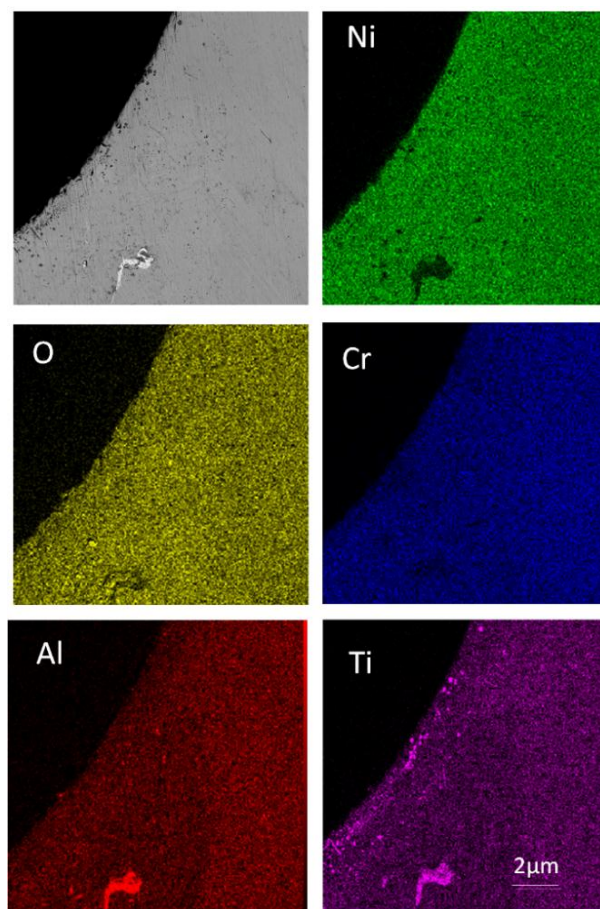

Figure 6. Elemental distribution maps of Ni, Cr, O, Ti, and Al within the region near the surface of a crack cleaned by 90 min FIC process

REFERENCES

1. Tao, P., Li, H., Huang, B., Hu, Q., Gong, S., Xu, Q., "The crystal growth, intercellular spacing and microsegregation of selective laser melted Inconel 718 superalloy", *Vacuum*, Vol. 159, (2019), 382-390. https://doi.org/10.1016/j.vacuum.2018.10.074
2. Naderi, M., Farvizi, M., Shirvani, K., Rahimipour, M. R., "Cyclic oxidation behavior of uncoated and aluminum-rich nickel aluminide coated Rene-80 superalloy", *Advanced Ceramics Progress*, Vol. 4, No. 3-4, (2018), 1-7. https://doi.org/10.30501/acp.2018.92925
3. Xiao, J., Prud'Homme, N., Li, N., Ji, V., "Influence of humidity on high temperature oxidation of Inconel 600 alloy: Oxide layers

and residual stress study", *Applied Surface Science*, Vol. 284, (2013), 446-452. https://doi.org/10.1016/j.apsusc.2013.07.117

4. Osoba, L. O., Oladoye, A. M., Ogbonna, V. E., "Corrosion evaluation of superalloys Haynes 282 and Inconel 718 in Hydrochloric acid", *Journal of Alloys and Compounds*, Vol. 804, (2019), 376-384. https://doi.org/10.1016/j.jallcom.2019.06.196

5. Seal, S., Kuiry, S. C., Bracho, L. A., "Studies on the surface chemistry of oxide films formed on IN-738LC superalloy at elevated temperatures in dry air", *Oxidation of Metals*, Vol. 56, No. 5, (2001), 583-603. https://doi.org/10.1023/a:1012569803467

6. Stankowski, A., "Advanced thermochemical cleaning procedures for structural braze repair techniques", *In Turbo Expo: Power for Land, Sea, and Air*, Vol. 36088, (2002), 1181-1195. https://doi.org/10.1115/gt2002-30535

7. Tarancon III, G., Midwest Inorganics LLC, "*Method for the Preparation of Anhydrous Hydrogen Halides, Inorganic Substances and/or inorganic Hydrides by Using as Reactants Inorganic Halides and reducing Agents*", U.S. Patent 8,834,830, (2014). https://patents.google.com/patent/US8834830B2/en

8. Wang, H., Liu, S., Li, B., Zhao, Z., "Characterization and removal of oxygen ions in LiF-NaF-KF melt by electrochemical methods", *Journal of Fluorine Chemistry*, Vol. 175, (2015), 28-31. https://doi.org/10.1016/j.jfluchem.2015.01.018

9. Kim, M. T., Chang, S. Y., Oh, O. Y., Won, J. B., "Fluoride ion cleaning of gas turbine components using PTFE grease", *Surface and Coatings Technology*, Vol. 200, No. 24, (2006), 6740-6748. https://doi.org/10.1016/j.surfcoat.2005.10.012

10. Miglietti, W., Blum, F., "Advantages of fluoride ion cleaning at sub-atmospheric pressure", *Engineering Failure Analysis*, Vol, 5, No. 2, (1998), 149-169. https://doi.org/10.1016/s1350-6307(98)00013-2

11. Sangeeta, D., General Electric Co, "*Method for Cleaning Cracks and Surfaces of Airfoils*", U.S. Patent 5,685,917, (1997). https://patents.google.com/patent/US5685917

12. Yin, H., Zhang, P., An, X., Cheng, J., Li, X., Wu, S., Wu, X., Liu, W., Xie, L., "Thermodynamic modeling of LiF-NaF-KF-CrF$_3$ system", *Journal of Fluorine Chemistry*, Vol. 209, (2018), 6-13. https://doi.org/10.1016/j.jfluchem.2018.02.005

13. Nicolaus, M., Möhwald, K., Maier, H. J., "Regeneration of high pressure turbine blades. Development of a hybrid brazing and aluminizing process by means of thermal spraying", *Procedia CIRP*, Vol. 59, (2017), 72-76. https://doi.org/10.1016/j.procir.2016.09.041

14. Hamidi, S., Rahimipour, M. R., Eshraghi, M. J., Hadavi, S. M. M., Esfahani, H., "Kinetics and Microstructural Investigation of High-Temperature Oxidation of IN-738LC Super Alloy", *Journal of Materials Engineering and Performance*, Vol. 26, No. 2, (2017), 563-570. https://doi.org/10.1007/s11665-016-2487-4

15. Wendt, H., Reuhl, K., Schwarz, V., "Cathodic deposition of refractory intermetallic compounds from flinak-melts—I. Voltammetric investigation of Ti, Zr, B, TiB$_2$ and ZrB$_2$", *Electrochimica Acta*, Vol. 37, No. 2, (1992), 237-244. https://doi.org/10.1016/0013-4686(92)85009-a

16. Ouyang, F. Y., Chang, C. H., You, B. C., Yeh, T. K., Kai, J. J., "Effect of moisture on corrosion of Ni-based alloys in molten alkali fluoride FLiNaK salt environments", *Journal of Nuclear Materials*, Vol. 437, No. 1-3, (2013), 201-207. https://doi.org/10.1016/j.jnucmat.2013.02.021

17. Esmaeili, H., Mirsalehi, S. E., Farzadi, A., "Vacuum TLP bonding of Inconel 617 superalloy using Ni-Cr-Si-Fe-B filler metal: metallurgical structure and mechanical properties", *Vacuum*, Vol. 152, (2018), 305-311. https://doi.org/10.1016/j.vacuum.2018.03.048

18. Singh, A. R. P., Nag, S., Hwang, J. Y., Viswanathan, G. B., Tiley, J., Srinivasan, R., Fraser, H. L., Banerjee, R., "Influence of cooling rate on the development of multiple generations of γ′ precipitates in a commercial nickel base superalloy", *Materials Characterization*, Vol. 62, No. 9, (2018), 878-886. https://doi.org/10.1016/j.matchar.2011.06.002

19. Shahbazi, M., Tayebifard, S. A., Razavi, M., "Effect of Ni content on the reaction behaviors and microstructure of TiB$_2$-TiC/Ni cermets synthesized by MASHS", *Advanced Ceramics Progress*, Vol. 2, No. 2, (2016), 22-26. https://doi.org/10.30501/acp.2016.70020

20. Zheng, L., Zhang, M., Dong, J., "Oxidation behavior and mechanism of powder metallurgy Rene95 nickel based superalloy between 800 and 1000 C", *Applied Surface Science*, Vol. 256, No. 24, (2010), 7510-7515. https://doi.org/10.1016/j.apsusc.2010.05.098

21. Doolabi, D. S., Rahimipour, M. R., Alizadeh, M., Pouladi, S., Hadavi, S. M. M., Vaezi, M. R., "Effect of high vacuum heat treatment on microstructure and cyclic oxidation resistance of HVOF-CoNiCrAlY coatings", *Vacuum*, Vol. 135, (2017), 22-33. https://doi.org/10.1016/j.vacuum.2016.10.014

22. Janz, G. J., Tomkins, R. P. T., "*Physical Properties Data Compilations Relevant to Energy Storage. IV. Molten Salts: Data on Additional Single and Multi-Component Salt Systems*", National Standard Reference Data System, National Bureau of Standards Report NSRDS-NBS 61 Part IV, U.S. Government Printing Office, Washington D.C., (1981). https://nvlpubs.nist.gov/nistpubs/Legacy/NSRDS/nbsnsrds61p4.pdf

23. Ye, X. X., Ai, H., Guo, Z., Huang, H., Jiang, L., Wang, J., Li, Z., Zhou, X., "The high-temperature corrosion of Hastelloy N alloy (UNS N10003) in molten fluoride salts analysed by STXM, XAS, XRD, SEM, EPMA, TEM/EDS", *Corrosion Science*, Vol. 106, (2016), 249-259. https://doi.org/10.1016/j.corsci.2016.02.010

24. Mantkowski, T. E., General Electric Co, "*Fluoride Ion Cleaning Method*", U.S. Patent 8,206,488, (2012). https://patents.google.com/patent/US8206488B2/en

25. Fritscher, K., "Life and FCT failure of yttria-and ceria-stabilized EBPVD TBC systems on Ni-base substrates", *Oxidation of Metals*, Vol. 91, No. 1, (2019), 131-157. https://doi.org/10.1007/s11085-018-9870-5

26. Williams, D. F., "*Assessment of Candidate Molten Salt Coolants for the NGNP/NHI Heat-Transfer Loop*", (No. ORNL/TM-2006/69). Oak Ridge National Lab.(ORNL), Oak Ridge, TN (United States), (2006). https://doi.org/10.2172/1360677

27. Acrivos, J., "Physical chemistry, Third Edition (Levine, Ira N.)", *Journal of Chemical Education*, Vol. 65, No. 12, (1988), A335. https://doi.org/10.1021/ed065pA335.3

28. Fukada, S., Morisaki, A., "Hydrogen permeability through a mixed molten salt of LiF, NaF and KF (Flinak) as a heat-transfer fluid", *Journal of Nuclear Materials*, Vol. 358, No. 2-3, (2006), 235-242. https://doi.org/10.1016/j.jnucmat.2006.07.011

29. Cruchley, S., Evans, H. E., Taylor, M. P., Hardy, M. C., Stekovic, S., "Chromia layer growth on a Ni-based superalloy: Sub-parabolic kinetics and the role of titanium", *Corrosion Science*, Vol. 75, (2013), 58-66. https://doi.org/10.1016/j.corsci.2013.05.016

30. Kool, L. B., Ritter, A. M., Cretegny, L., Pezzutti, M. D., Beitz, S. W., General Electric Co, "*Method for Removing Oxide from Cracks in Turbine Components*", U.S. Patent 7,125,457, (2006). https://patents.google.com/patent/US7125457B2/en